

Blood flow analysis with considering nanofluid effects in vertical channel

S. Noreen¹ · M. M. Rashidi^{2,3} · M. Qasim¹

Received: 1 March 2017 / Accepted: 13 April 2017 / Published online: 25 April 2017
© The Author(s) 2017. This article is an open access publication

Abstract Manipulation of heat convection of copper particles in blood has been considered peristaltically. Two-phase flow model is used in a channel with insulating walls. Flow analysis has been approved by assuming small Reynold number and infinite length of wave. Coupled equations are solved. Numerical solution are computed for the pressure gradient, axial velocity function and temperature. Influence of attention-grabbing parameters on flow entities has been analyzed. This study can be considered as mathematical representation to the vibrance of physiological systems/tissues/organs provided with medicine.

Keywords Copper nanoparticles · Pseudoplastic fluid · Heat convection · Viscous dissipation

Introduction

Fluids are mostly used as energy (heat) carriers. For efficient heat transfer, low thermal conductivity of fluid is major constraint. As a result, engineering fluids are developed with suspensions of metallic particles. The word nanofluid was initially used by Choi (1995). Fluids like

water, engine oil, ethylene glycol, some lubricants, blood and polymer solutions have low thermal conductivity as compared to solids. By adding solid particles of higher thermal conductivity to these fluid, raises the thermal conductivity of these fluids. These solid particles are usually of the size of the order of 1–100 nanometers and known as nanoparticles are mostly of materials, such as metals (Ag, Au, Cu, Fe), nitride ceramics (AlN, SiN), oxide ceramics (Al₂O₃, CuO), carbide ceramics (SiC, TiC), semiconductors (TiO₂) and single-, double- or many-walled carbon nanotubes (DWCNT, SWCNT, MWCNT). The base fluids in which these particles are added are termed as nanofluids. Nanofluids carry up to a 5% volume fraction ϵ of nanoparticles to guarantee effective heat transfer enhancement. The nanofluid is composed of three different types of magnetic (cobalt ferrite CoFe₂O₄, magnetite Fe₃O₄, and Mn–Zn ferrite Mn–ZnFe₂O₄) and non-magnetic (silver Ag, alumina Al₂O₃ and titania TiO₂) nanoparticles (Khan et al. 2014; Sheikholeslami et al. 2016; Sheikholeslami and Rashidi 2015; Malvandi and Ganji 2016; Hussanan and Salleh 2017).

Fluid flows driven by heat convection in open channels have been in progress, over the past few decades, for vertical or inclined geometries. This great interest stems from its range of utilizations, such as the chilling of electronic devices, solar chimney, solar cells, solar energy collectors and as a means of facilitating thermal performance in many other industrial processes. Flows induced by travelling sinusoidal waves on channel walls are referred as peristaltic flows. The peristaltic transport has fundamental importance due to physiological and many other applications such as urine transportation, chyme motion, spermatozoa transport, vasomotion of small blood vessels, heart–lung machine, sanitary fluid transport, hose pumps, dialysis machine, and transport of corrosive fluids in

✉ S. Noreen
laurel_lichen@yahoo.com

¹ Department of Mathematics, COMSATS Institute of Information Technology, Park Road, Islamabad 44000, Pakistan

² Shanghai Key Lab of Vehicle Aerodynamics and Vehicle Thermal Management Systems, Tongji University, 4800 Cao An Rd., Jiading, Shanghai 201804, China

³ ENN-Tongji Clean Energy Institute of Advanced Studies, Shanghai, China

nuclear industry. Earthworms use similar system to derive their locomotion. Modern machinery imitate this design like robots. Latham (1966) was the first who discussed the peristaltic theory of viscous fluid. Meanwhile, Shapiro (1969) analyzed the peristaltic transport of viscous fluid experimentally. Afterwards, several investigators made significant researches in peristalsis by accounting various geometries and suppositions (Kothandapani and Srinivas 2008; Mekheimer and Abd elmaboud 2008; Srinivas and Kothandapani 2008; Gnanaswara et al. 2016; Asghar and Ali 2016; Ali et al. 2016; Noreen et al. 2015; Nowar 2014; Sarkar et al. 2015; Mekheimer and Abd Elmaboud 2015).

Adjacent to this, non-Newtonian fluids are habitually used for flow of alloys/metals and blood flow at low shear rate. Here heating traits in non-Newtonian fluids are inevitable. Heat transfer through nanofluid involves destruction of undesirable cancer tissues. Researches additionally trimmed down for the case of non-Newtonian fluids with nanoparticles (Noreen 2013; Reddy and Makinde 2016; Abou-zeid 2016; Mekheimer 2016; Kothandapani and Prakash 2016a, b). Excessive copper deposits in the human body is not a big deal. One omission is “Wilson’s syndrome. A number of people are born disable to remove copper from their bodies. Copper preserves in them. Excessive reservoir of copper in human body can affect a person’s liver/brain/kidneys. Worse effects include mental illness/death. Luckily, this issue can be fixed. Patients are provided with chemical that combines with copper, and that is how copper’s spoiling effects on the body are narrowed down. Present article endeavor more in this course.

This work for the first time, evaluates the nano effects of copper particles on peristaltic transport of blood in the presence of heat convection. Current article aims to identify the influence of copper particles in the motion of blood in a vertical channel, and then to define modelling of blood by a non-Newtonian shear thinning fluid (Boger 1977) (considering pseudoplastic fluid as blood makes the problem more general. Such consideration is important in medical science), the detailed description of the mathematical formulation with mixed convection in vertical channels provides complete analysis of this topic in section two. Discussion of graphical results is done in division three. Conclusions are explored in division four.

Problem development and formulation

Let us consider a two-dimensional incompressible flow of copper-blood nanofluid in an asymmetric channel of thickness $d_1 + d_2$. Pseudoplastic fluid is used to represent rheology of blood. Motion is induced by sinusoidal wave

moving with speed c channel boundaries. Coordinates system (\bar{X}, \bar{Y}) with \bar{X} parallel and \bar{Y} perpendicular to the course of wave is projected. The wave geometry is taken as

$$\begin{aligned} \bar{h}_1(\bar{X}, \bar{t}) &= \bar{a}_1 \cos\left(\frac{2\pi}{\lambda}(\bar{X} - c\bar{t})\right) + \bar{d}_1, & \text{upper wall,} \\ \bar{h}_2(\bar{X}, \bar{t}) &= -\bar{b}_1 \cos\left(\frac{2\pi}{\lambda}(\bar{X} - c\bar{t}) + \Omega\right) - \bar{d}_2 & \text{lower wall,} \end{aligned} \quad (1)$$

where phase difference Ω varies in the limit $0 \leq \Omega \leq \pi$ and \bar{a}_1, \bar{b}_1 are the amplitudes of travelling waves. The case $\Omega = 0$ matches to the symmetric channel. Additionally, \bar{t} the time, λ is the wavelength. Symbolizing components \bar{U} and \bar{V} in \bar{X} and \bar{Y} -directions in the fixed frame, the velocity field \mathbf{V} is

$$\mathbf{V} = [\bar{U}(\bar{X}, \bar{Y}, \bar{t}), \bar{V}(\bar{X}, \bar{Y}, \bar{t}), 0]. \quad (2)$$

The governing equations for the present flow problem are:

$$\nabla \cdot \mathbf{V} = 0, \quad (3)$$

$$\rho_{\text{ef}} \frac{d\mathbf{V}}{dt} = \text{div} \mathbf{T} + \mathbf{g}(\rho\beta)_{\text{ef}}(T - T_0), \quad (4)$$

$$(\rho C)_{\text{ef}} \frac{dT}{dt} = \kappa_{\text{ef}} \nabla^2 T + \mathbf{T} \cdot \mathbf{L}. \quad (5)$$

Here T the temperature, d/dt the material derivative. For copper-blood nanofluid ρ_{ef} is the effective density, C_p the specific heat, and κ_{ef} the effective thermal conductivity are adopted in the following form:

$$(\rho C)_{\text{ef}} = (1 - \epsilon)(\rho C)_f + \epsilon(C\rho)_p, \quad (6)$$

$$\rho_{\text{ef}} = (1 - \epsilon)\rho_f + \epsilon\rho_p, \quad (7)$$

$$(\rho\beta)_{\text{ef}} = (1 - \epsilon)(\rho\beta)_f + \epsilon(\rho\beta)_p$$

$$k_{\text{ef}} = \frac{2k_f + k_p + 2\epsilon(k_p - k_f)}{2k_f + k_p - \epsilon(k_p - k_f)} k_f \quad (8)$$

$$\mu_{\text{ef}} = \frac{1}{(1 - \epsilon)^{2.5}} \quad (9)$$

where f and p , respectively, refer to fluid and nanoparticle, ρ_f is the density of the base fluid, ρ_p is the density of the nanoparticle, k_f is the fluid thermal conductivity, k_p is the thermal conductivity of the nanoparticles, and C_p and C_f are the heat capacities of the nanoparticle and the base fluid, respectively, and ϵ is the volume fraction of the nanoparticles. This is also known as Brinkmann model.

Cauchy stress tensor for pseudoplastic fluid is Boger (1977)

$$\bar{\mathbf{T}} = \bar{\mathbf{S}} - p\bar{\mathbf{I}}, \quad (10)$$

$$\bar{\lambda}_1 \bar{\mathbf{S}}^\nabla + \bar{\mathbf{S}} + \frac{1}{2}(\bar{\mathbf{A}}_1 \bar{\mathbf{S}} + \bar{\mathbf{S}} \bar{\mathbf{A}}_1)(\bar{\lambda}_1 - \bar{\mu}_1) = \mu \bar{\mathbf{A}}_1, \quad (11)$$

$$\bar{\mathbf{S}}^\nabla = -\bar{\mathbf{S}}\bar{\mathbf{L}}^T + \frac{d\bar{\mathbf{S}}}{dt} - \bar{\mathbf{L}}\bar{\mathbf{S}}, \quad \bar{\mathbf{L}} = \nabla\bar{\mathbf{V}}, \tag{12}$$

in which $\bar{\mathbf{I}}$ identity tensor, $\bar{\mathbf{S}}$ extra stress tensor, μ dynamic viscosity, p pressure, $\bar{\mathbf{S}}^\nabla$ upper-convected derivative and $\bar{\mu}_1$ and $\bar{\lambda}_1$ represents relaxation times. Introducing the transformations

$$\begin{aligned} \xi &= \bar{X} - c\bar{t}, \quad \eta = \bar{Y}, \\ \bar{u}(\bar{\xi}, \bar{\eta}) &= \bar{U} - c, \quad \bar{v}(\bar{\xi}, \bar{\eta}) = \bar{V}, \end{aligned} \tag{13}$$

Equations (1)–(12) in terms of above transformations give

$$\frac{\partial \bar{u}}{\partial \bar{\xi}} + \frac{\partial \bar{v}}{\partial \bar{\eta}} = 0, \tag{14}$$

$$\begin{aligned} \rho_{\text{ef}} \left((\bar{u} + c) \frac{\partial}{\partial \bar{\xi}} + \bar{v} \frac{\partial}{\partial \bar{\eta}} \right) (\bar{u} + c) + \frac{\partial \bar{p}}{\partial \bar{\xi}} &= \frac{\partial \bar{S}_{\bar{\xi}\bar{\xi}}}{\partial \bar{\xi}} + \frac{\partial \bar{S}_{\bar{\xi}\bar{\eta}}}{\partial \bar{\eta}} \\ &+ g(\rho\beta)_{\text{ef}}(\bar{T} - T_0) \end{aligned} \tag{15}$$

$$\rho_{\text{ef}} \left((\bar{u} + c) \frac{\partial}{\partial \bar{\xi}} + \bar{v} \frac{\partial}{\partial \bar{\eta}} \right) \bar{v} + \frac{\partial \bar{p}}{\partial \bar{\eta}} = \frac{\partial \bar{S}_{\bar{\xi}\bar{y}}}{\partial \bar{\xi}} + \frac{\partial \bar{S}_{\bar{\eta}\bar{\eta}}}{\partial \bar{\eta}}, \tag{16}$$

$$\begin{aligned} (\rho C_p)_{\text{ef}} \left[(\bar{u} + c) \frac{\partial}{\partial \bar{\xi}} + \bar{v} \frac{\partial}{\partial \bar{\eta}} \right] \bar{T} &= \kappa_{\text{ef}} \left[\frac{\partial^2 \bar{T}}{\partial \bar{\xi}^2} + \frac{\partial^2 \bar{T}}{\partial \bar{\eta}^2} \right] \\ &+ \bar{S}_{\bar{\xi}\bar{\xi}} \frac{\partial \bar{u}}{\partial \bar{\xi}} + \bar{S}_{\bar{\eta}\bar{\eta}} \frac{\partial \bar{v}}{\partial \bar{\eta}} + \bar{S}_{\bar{\xi}\bar{\eta}} \left[\frac{\partial \bar{v}}{\partial \bar{\xi}} + \frac{\partial \bar{u}}{\partial \bar{\eta}} \right], \end{aligned} \tag{17}$$

Defining dimensionless wave (δ), Prandtl (Pr), Reynolds (Re), Eckert (Ec), amplitude ratio (α), temperature (Π), stream function (ψ), relaxation times (λ_1, μ_1), and wall temperature (T_0, T_1):

$$\begin{aligned} \lambda_1 &= \frac{\bar{\lambda}_1 c}{a}, \quad \xi = \frac{\bar{\xi}}{\lambda}, \quad y = \frac{\bar{y}}{a}, \quad t = \frac{c\bar{t}}{\lambda}, \quad p = \frac{a^2 \bar{p}}{c\lambda\mu}, \\ u &= \frac{\bar{u}}{c}, \quad v = \frac{\bar{v}}{c}, \quad Gr = \frac{\rho_f g \beta_f T_0 a^2}{c\mu_f} \\ \delta &= \frac{a}{\lambda}, \quad \bar{S}_{ij} = \frac{a\bar{S}_{ij}}{\mu_f c} \quad (\text{for } i, j = 1, 2, 3), \quad \mu_1 = \frac{\bar{\mu}_1 c}{a}, \end{aligned} \tag{18}$$

$$\begin{aligned} \Pi &= \frac{\bar{T} - T_0}{T_1 - T_0}, \quad Re = \frac{c\rho_f}{\mu_f} \\ Ec &= \frac{c^2}{(C)_f(T_1 - T_0)}, \quad Pr = \frac{\mu_{\text{ef}}(C_p)_f}{\kappa_{\text{ef}}}, \quad b = \frac{\bar{b}_1}{d_1}, \\ h_1 &= \frac{\bar{h}_1}{d_1}, \quad h_2 = \frac{\bar{h}_2}{d_1}, \quad a = \frac{\bar{a}_1}{d_1}, \end{aligned}$$

the wall surfaces are

$$\begin{aligned} h_1 &= 1 + a \cos(2\pi\xi), \\ h_2 &= -d - b \cos(2\pi\xi + \Omega). \end{aligned} \tag{19}$$

Introducing

$$v = -\delta \frac{\partial \Psi}{\partial \xi}, \quad u = \frac{\partial \Psi}{\partial \eta}, \tag{20}$$

continuity equation (14) is identically satisfied and Eqs. (15)–(17) yield

$$\begin{aligned} -Re\delta^3 \left((1 - \phi_1) + \frac{\phi_1 \rho_p}{\rho_f} \right) &\left(-\left(\frac{\partial \Psi}{\partial \eta} + 1 \right) \frac{\partial^2 \Psi}{\partial \xi^2} + \frac{\partial \Psi}{\partial \xi} \frac{\partial^2 \Psi}{\partial \eta \partial \xi} \right) \\ &= -\frac{\partial p}{\partial \eta} - \frac{\delta^2}{K(1 - \phi_1)^{2.5}} + \frac{\delta}{(1 - \phi_1)^{2.5}} \left(-\delta^2 \frac{\partial^3 \Psi}{\partial \xi^3} - \delta \frac{\partial^3 \Psi}{\partial \xi \partial \eta^2} \right) \end{aligned} \tag{21}$$

$$\begin{aligned} Re\delta \left((1 - \epsilon) + \frac{\epsilon \rho_p}{\rho_f} \right) &\left(\left(\frac{\partial \Psi}{\partial \eta} + 1 \right) \frac{\partial^2 \Psi}{\partial \xi \partial \eta} - \frac{\partial \Psi}{\partial \xi} \frac{\partial^2 \Psi}{\partial \eta^2} \right) + \frac{\partial p}{\partial \xi} \\ &= \frac{\partial S_{\xi\eta}}{\partial \eta} + Gr \left[(1 - \epsilon) + \epsilon \left(\frac{\rho\beta}{(\rho\beta)_f} \right) \right] \Pi + \delta \frac{\partial S_{\xi\xi}}{\partial \xi} \end{aligned} \tag{22}$$

$$\begin{aligned} -Re\delta^2 \left((1 - \epsilon) + \frac{\epsilon \rho_p}{\rho_f} \right) &\left(\frac{\partial \Psi}{\partial \eta} \frac{\partial}{\partial \xi} - \frac{\partial \Psi}{\partial \xi} \frac{\partial}{\partial \eta} \right) \frac{\partial \Psi}{\partial \xi} + \frac{\partial p}{\partial \eta} \\ &= \delta \left(\delta \frac{\partial S_{\eta\xi}}{\partial \xi} + \frac{\partial S_{\eta\eta}}{\partial \eta} \right), \end{aligned} \tag{23}$$

$$\begin{aligned} c\delta d_1(1 - \phi_1)(\rho c)_f + \phi_1(\rho C)_p &\left[\left(\frac{\partial \Psi}{\partial \eta} + 1 \right) \frac{\partial \Pi}{\partial \xi} - \frac{\partial \Psi}{\partial \xi} \frac{\partial \Pi}{\partial \eta} \right] \\ &= K_{\text{eff}} \delta^2 \frac{\partial^2 \Pi}{\partial \xi^2} + \frac{\partial^2 \Pi}{\partial \eta^2} + Ec Pr \frac{1}{(1 - \epsilon)^{2.5}} \\ &\times \delta (S_{xx} - S_{\eta\eta}) \frac{\partial^2 \Psi}{\partial \xi \partial \eta} + \left(\frac{\partial^2 \Psi}{\partial \eta^2} - \delta^2 \frac{\partial^2 \Psi}{\partial \xi^2} \right) S_{\xi\eta} \end{aligned} \tag{24}$$

$$\begin{aligned} \frac{1}{(1 - \epsilon)^{2.5}} \left(2\delta \frac{\partial^2 \Psi}{\partial \eta \partial \xi} \right) &= S_{\xi\xi} + \lambda_1 \left[\left(\delta \frac{\partial \Psi}{\partial \eta} \frac{\partial}{\partial \xi} + \frac{\partial \Psi}{\partial \xi} \frac{\partial}{\partial \eta} \right) \right. \\ &S_{\xi\xi} - 2 \left(\delta \frac{\partial^2 \Psi}{\partial \xi \partial \eta} S_{xx} + \frac{\partial^2 \Psi}{\partial \eta^2} S_{\xi\eta} \right) \\ &\left. + \frac{1}{2}(\lambda_1 - \mu_1) \left(4\delta S_{\xi\xi} \frac{\partial^2 \Psi}{\partial \xi \partial \eta} + 2S_{\xi\eta} \left(\frac{\partial^2 \Psi}{\partial \eta^2} - \delta^2 \frac{\partial^2 \Psi}{\partial \xi^2} \right) \right) \right], \end{aligned} \tag{25}$$

$$\begin{aligned} -\frac{1}{(1 - \epsilon)^{2.5}} \left(2\delta \frac{\partial^2 \Psi}{\partial \eta \partial \xi} \right) \\ &= S_{\eta\eta} + \lambda_1 \left[\delta \left(\frac{\partial \Psi}{\partial \eta} \frac{\partial}{\partial \xi} - \frac{\partial \Psi}{\partial \xi} \frac{\partial}{\partial \eta} \right) S_{\eta\eta} + 2\delta \left(\delta \frac{\partial^2 \Psi}{\partial \xi^2} S_{\xi\eta} + \frac{\partial^2 \Psi}{\partial \xi \partial \eta} S_{\eta\eta} \right) \right. \\ &\left. + \frac{1}{2}(\lambda_1 - \mu_1) \left[2S_{\xi\eta} \left(\frac{\partial^2 \Psi}{\partial \eta^2} - \delta^2 \frac{\partial^2 \Psi}{\partial \xi^2} \right) - 4\delta S_{yy} \frac{\partial^2 \Psi}{\partial \xi \partial \eta} \right] \right], \end{aligned} \tag{26}$$

$$\begin{aligned} \frac{1}{(1 - \epsilon)^{2.5}} \left(\frac{\partial^2 \Psi}{\partial \eta^2} - \delta^2 \frac{\partial^2 \Psi}{\partial \xi^2} \right) \\ &= +\lambda_1 \left[\delta \left(\frac{\partial \Psi}{\partial \eta} \frac{\partial}{\partial \xi} - \frac{\partial \Psi}{\partial \xi} \frac{\partial}{\partial \eta} \right) S_{\xi\eta} - \left(\frac{\partial^2 \Psi}{\partial \eta^2} S_{\eta\eta} - \delta^2 \frac{\partial^2 \Psi}{\partial \xi^2} S_{xx} \right) \right] \\ &+ S_{\xi\eta} + \frac{1}{2}(\lambda_1 - \mu_1) \left[(S_{xx} + S_{\eta\eta}) \left(\frac{\partial^2 \Psi}{\partial \eta^2} - \delta^2 \frac{\partial^2 \Psi}{\partial \xi^2} \right) \right]. \end{aligned} \tag{27}$$

Assuming that peristaltic wave is of infinite length

$$\frac{\partial p}{\partial \xi} = \frac{1}{(1 - \epsilon)^{2.5}} \frac{\partial S_{\xi\eta}}{\partial y} + Gr \left[(1 - \epsilon) + \epsilon \left(\frac{(\rho\beta)_p}{(\rho\beta)_f} \right) \right] \Pi, \tag{28}$$

$$\frac{\partial p}{\partial \eta} = 0, \tag{29}$$

$$\left(\frac{k_p + 2k_f + 2\epsilon(k_p - k_f)}{k_p + 2k_f - \epsilon(k_p - k_f)} \right) \frac{\partial^2 \gamma}{\partial \eta^2} + Br \frac{1}{(1 - \epsilon)^{2.5}} \frac{\partial^2 \Psi}{\partial \eta^2} S_{\xi\eta} = 0, \tag{30}$$

$$S_{\xi\xi} = (\lambda_1 + \mu_1) \frac{\partial^2 \Psi}{\partial \eta^2} S_{\xi\eta}, \tag{31}$$

$$S_{\eta\eta} = (-\lambda_1 + \mu_1) S_{\xi\eta} \frac{\partial^2 \Psi}{\partial \eta^2}, \tag{32}$$

$$(1 - \epsilon)^{2.5} S_{\xi\eta} = \frac{\Psi_{yy}}{1 + \chi \Psi_{\eta\eta}^2}, \tag{33}$$

with $(\lambda_1^2 - \mu_1^2) = \chi$.

The conditions at boundary in wave frame are

$$\Psi = \frac{F}{2}, \frac{\partial \Psi}{\partial \eta} = -1, \quad \Pi = 0 \quad \text{at} \quad \eta = h_1, \tag{34}$$

$$\Psi = -\frac{F}{2}, \frac{\partial \Psi}{\partial \eta} = -1, \quad \Pi = 1 \quad \text{at} \quad \eta = h_2$$

where F (dimensionless time mean flow rate in moving frame) and g (dimensionless time mean flow rate in the fixed frame) are equated by $g = F + 1 + d$ with

$$F = \int_{h_2}^{h_1} \frac{\partial \Psi}{\partial \eta} d\eta. \tag{35}$$

Employing Eqs. (28) and (33), one obtains

$$\frac{\partial p}{\partial \xi} = \frac{1}{(1 - \epsilon)^{2.5}} \frac{\partial}{\partial \eta} \left[\Psi_{\eta\eta} \left\{ 1 - \chi \left(\frac{\partial^2 \Psi}{\partial \eta^2} \right)^2 \right\} \right] + Gr \left[(1 - \epsilon) + \epsilon \left(\frac{(\rho\beta)_p}{(\rho\beta)_f} \right) \right] \Pi, \tag{36}$$

Equations (29) and (36) yield

$$\frac{1}{(1 - \epsilon)^{2.5}} \frac{\partial^4 \Psi}{\partial \eta^4} - \chi \frac{1}{(1 - \epsilon)^{2.5}} \frac{\partial^2}{\partial \eta^2} \left(\frac{\partial^2 \Psi}{\partial \eta^2} \right)^3 + Gr \left[(1 - \epsilon) + \epsilon \left(\frac{(\rho\beta)_p}{(\rho\beta)_f} \right) \right] \frac{\partial \Pi}{\partial \eta} = 0. \tag{37}$$

Pressure rise ΔP_λ

$$\Delta P_\lambda = \int_0^1 \frac{dp}{d\xi} d\xi. \tag{38}$$

Results and discussion

A comparison of considered thermophysical characteristics of base fluid and nanoparticles is stated in Table 1. In this section, we have analyzed the obtained numerical results. Flow of pseudoplastic fluid with copper nanoparticles is studied. Copper is well-known thermal and electrical conductor making it ideal for markable electrical purposes. To study the influence of Grashof number Gr , relaxation time χ and volume fraction of copper nanoparticles ϵ , the velocity u , pressure ΔP_λ and temperature Π are graphically explored in Figs. 1, 2, 3, 4, 5, 6, 7, 8, 9 and 10.

Table 1 Thermophysical properties of base fluid and nanoparticles

Physical properties	Base fluid	Copper particles
ρ (kg/m ³)	1025	8933
K (W/mK)	0.52	401
β (1/K) $\times 10^{-6}$	0.004	16.65

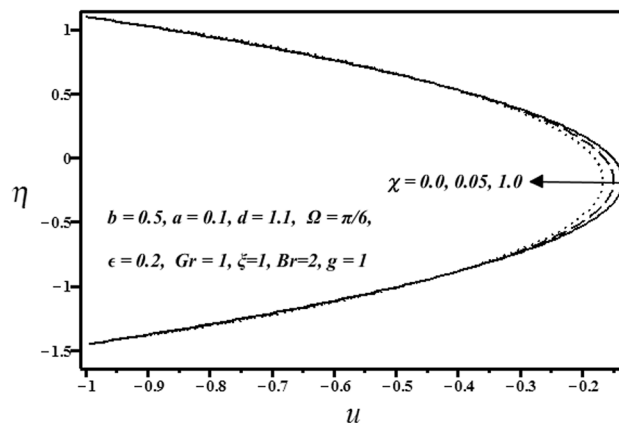


Fig. 1 Influence of χ on u

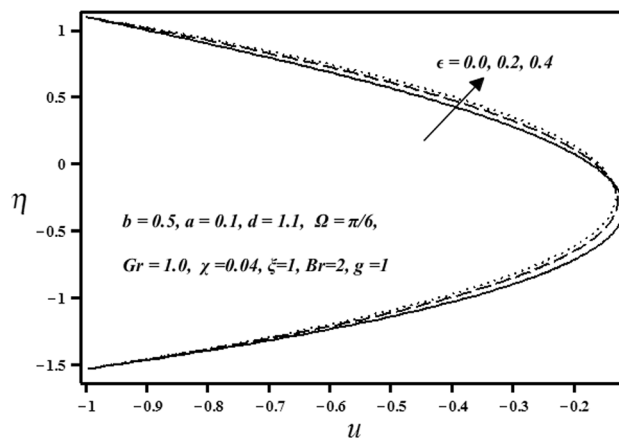


Fig. 2 Influence of ϵ on u

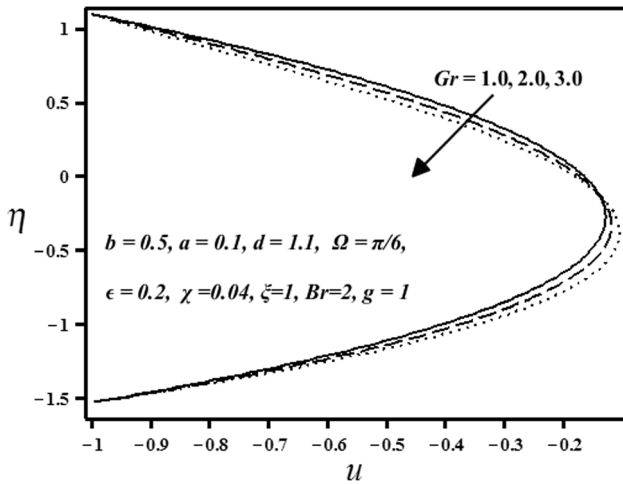


Fig. 3 Influence of Gr on u

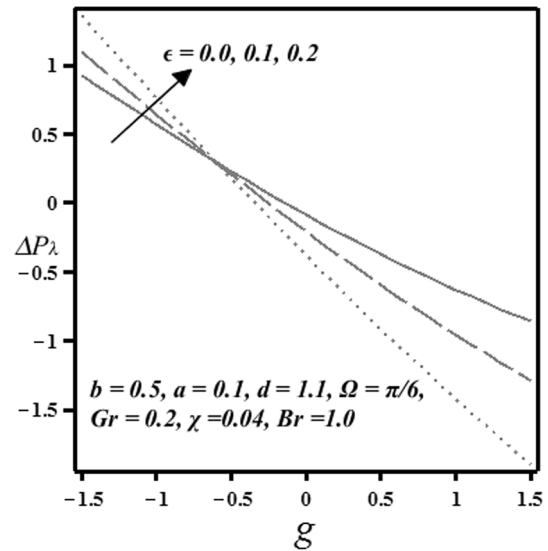


Fig. 5 Influence of ϵ on ΔP_λ

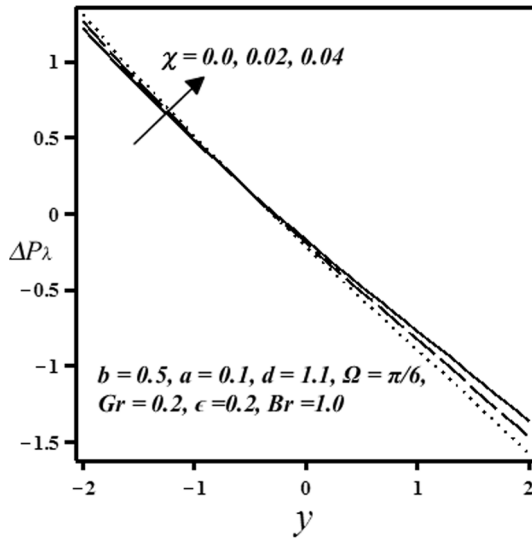


Fig. 4 Influence of χ on ΔP_λ

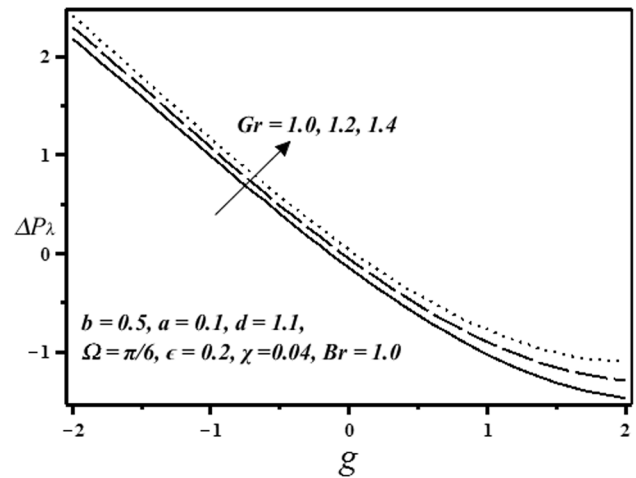


Fig. 6 Influence of Gr on ΔP_λ

Figure 1 depict the behavior of velocity for different values of the non-Newtonian fluid parameter χ . It is observed that velocity profile is parabolic and its magnitude is maximum near the center of the channel. It is noticed that the velocity decreases by increasing the fluid parameter χ . Figure 2 examined the impact of copper nanoparticles. It is noticed that magnitude of velocity decreases above the centerline with an increase in the value of ϵ . Copper particles concentration provide a resistance to flow, and thus hinders fluid from attaining high velocities at $\eta = 0$. Velocity at channel center and wall is dissimilar. Natural tendency of fluid to migrate due to some driving force of buoyancy caused by a temperature gradient is explained by Grashof number Gr . The variations of Gr on the velocity is conspired in Fig. 3 by fixing values of $a = 0.1, b = 0.5, \phi = \pi/6$ and $d = 1.1$. In Fig. 3 it is discovered that the magnitude of velocity increases in region

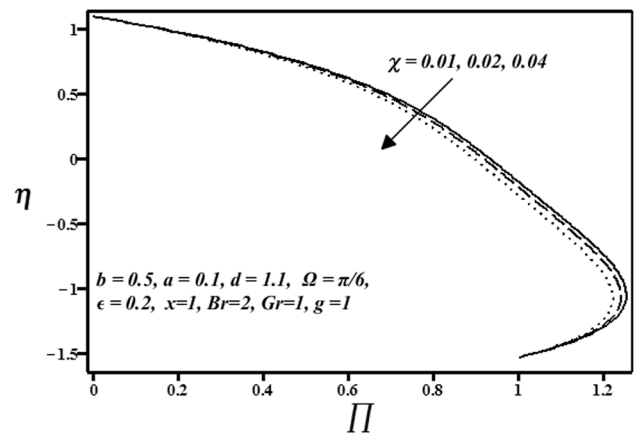


Fig. 7 Influence of χ on Π

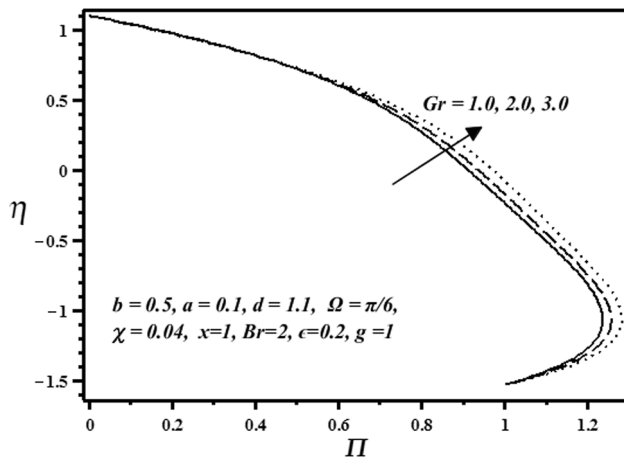


Fig. 8 Influence of ϵ on Π

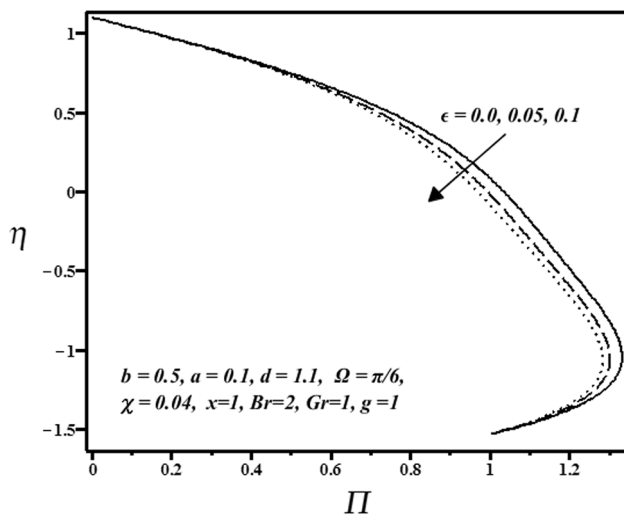


Fig. 9 Influence of Gr on Π

$0 \leq \eta \leq 1.1$ and it decreases in region $-1.6 \leq \eta \leq 0$ with a raise in Gr .

Rise in pressure per wavelength against volume flow rate g is portrayed in Figs. 4, 5 and 6. Effect of ϵ on ΔP_λ is seen

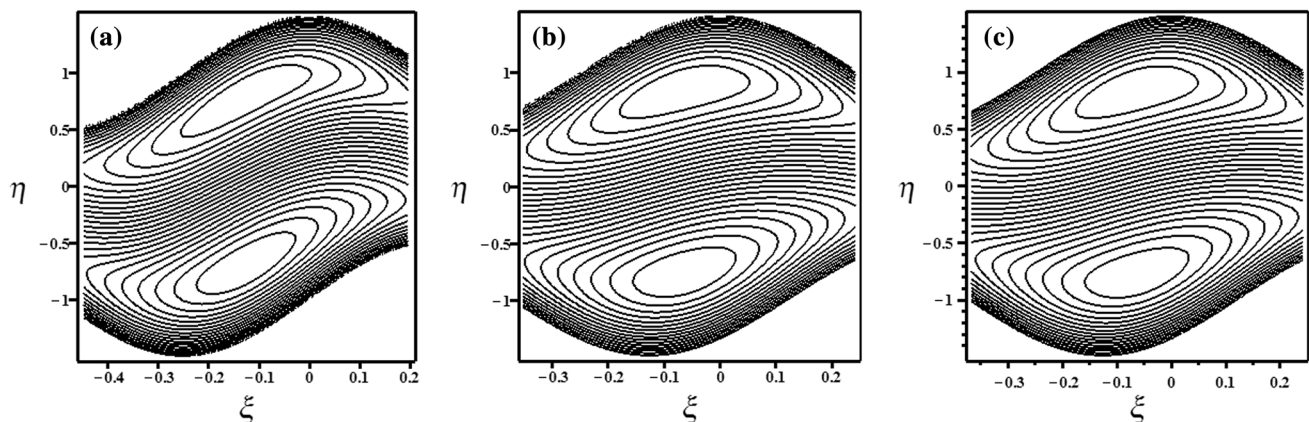


Fig. 10 **a** Streamlines for $\epsilon = 0.0$. **b** Streamlines for $\epsilon = 0.1$. **c** Streamlines for $\epsilon = 0.2$

in Fig. 4. Copper has demonstrated its antimicrobial effectiveness in biological engineering. The effectiveness of copper and copper alloys as antimicrobial coatings on touch-surfaces has been well documented by many researchers. Here in pumping ($\Delta P_\lambda > 0$) and free ($\Delta P_\lambda = 0$) pumping section, the pumping rate enhances by rising nanoparticle volume fraction ϵ . Whereas in the co-pumping section $\Delta P_\lambda < 0$, the pumping rate lessen down by increasing ϵ . It is found from Figs. 5 and 6 that Δp_λ is growing function of fluid parameter χ and Grashof (Gr) number.

Figures 7, 8 and 9 explained the temperature distribution Π of fluid for the significant parameters. The effect of χ on distribution Π has been described in Fig. 7. Obviously, the magnitude of Π decreases when χ is increased. Figures 8 and 9 that the value of temperature distribution Π is boosted with Gr and dropped off upon increasing ϵ . Hence, the totting of copper nanoparticle volume fraction, increases heat loss of fluid. High thermal conductivity of copper is the foremost reason behind it.

Figure 10 has demonstrated trapping analysis. Streamlines indicated the paths of fluid units in a flow regime. The development of inner mingling fluid bolus by the sealed streamlines is trapping. Flow went through a bifurcation process which has resulted in bolus. The streamlines are shown for the variations of copper particle concentration from 0, 10 and 20 cent in the pseudoplastic fluid. These figures indicate that the dimension of trapped bolus diminishes by enhancing concentration of nanoparticles. The number of closed circulating streamlines also increases.

Conclusions

The study inspects the manipulation of copper particles and heat convection on peristaltically moving pseudoplastic fluid. Two-phase flow model is used. We specifically note the following results:

1. Pumping rate increases with χ and Gr and decreases with ϵ for copper-blood fluid flow.
2. The velocity profile has differing behavior around walls h_1 and h_2 with an increase in Gr .
3. Trapping is likely perturbed by increasing concentration of copper particles in pseudoplastic fluid.
4. Concentration of copper nanoparticles disfavors the maximum velocity u in pseudoplastic fluid.
5. Gr parameter increases temperature distribution Π in copper-blood fluid flow.
6. Addition of copper prevents overheating.

Open Access This article is distributed under the terms of the Creative Commons Attribution 4.0 International License (<http://creativecommons.org/licenses/by/4.0/>), which permits unrestricted use, distribution, and reproduction in any medium, provided you give appropriate credit to the original author(s) and the source, provide a link to the Creative Commons license, and indicate if changes were made.

References

- Abou-zeid Mohamed (2016) Effects of thermal-diffusion and viscous dissipation on peristaltic flow of micropolar non-Newtonian nanofluid: application of homotopy perturbation method. *Results Phys* 6:481–495
- Ali N, Abbasi A, Ahmad I (2016) Channel flow of Ellis fluid due to peristalsis. *AIP Adv* 5:097214. doi:10.1063/1.4932042
- Asghar Z, Ali N (2016) Analysis of mixed convective heat and mass transfer on peristaltic flow of Fene-P fluid with chemical reaction. *J Mech* 32:83–92
- Boger DV (1977) Demonstration of upper and lower Newtonian fluid behavior in a pseudoplastic fluid. *Nature* 265:126–128
- Choi SUS (1995) Enhancing thermal conductivity of fluids with nanoparticles. *ASME Fluids Eng Div* 231:99–105
- Ganeswara Reddy M, Venugopal Reddy K, Makinde OD (2016) Hydromagnetic peristaltic motion of a reacting and radiating couple stress fluid in an inclined asymmetric channel filled with a porous medium. *Alex Eng J* 55:1841–1853
- Hussanan A, Salleh MZ, Khan I, Shafie Sharidan (2017) Convection heat transfer in micropolar nanofluids with oxide nanoparticles in water, kerosene and engine oil. *J Mol Liq* 229:482–488
- Khan ZH, Khan WA, Qasim M, Shah IA (2014) MHD stagnation point ferrofluid flow and heat transfer toward a stretching sheet. *IEEE Trans Nanotechnol* 13:35–40
- Kothandapani M, Prakash J (2016) Influences of chemical reaction and convective boundary conditions on the Peristaltic transport of MHD Jeffery nanofluids. *J Nanofluids* 5:790–801
- Kothandapani M, Prakash J (2016) Convective boundary conditions effect on peristaltic flow of a MHD Jeffery nanofluid. *Appl Nanosci* 6:323–335
- Kothandapani M, Srinivas S (2008) Nonlinear peristaltic transport of a Newtonian fluid in an inclined asymmetric channel through a porous medium. *Phys Lett A* 372:1265–1276
- Latham TW (1966) Fluid motion in a peristaltic pump. MIT Cambridge, Cambridge
- Malvandi A, Ganji DD (2016) Mixed convection of alumina/water nanofluid in microchannels using modified Buongiorno's model in presence of heat source/sink. *J Appl Fluid Mech* 9:2277–2289
- Mekheimer KhS, Elnaqeeb T, El Kot MA, Alghamdi F (2016) Simultaneous effect of magnetic field and metallic nanoparticles on a micropolar fluid through an overlapping stenotic artery: blood flow model. *Phys Essays* 29:272–283
- Mekheimer KS, Abd Elmaboud Y (2008) Peristaltic flow of a couple stress fluid in an annulus: application of an endoscope. *Physica A* 387:2403–2415
- Mekheimer KhS, Abd Elmaboud Y (2015) Simultaneous effects of variable viscosity and thermal conductivity on peristaltic flow in a vertical asymmetric channel. *Can J Phys* 92:1541–1555
- Noreen S (2013) Mixed convection peristaltic flow of third order nanofluid with an induced magnetic field. *PLoS One* 8(11):e78770
- Noreen S, Qasim M, Khan ZH (2015) MHD pressure driven flow of nanofluid in curved channel. *J Magn Magn Mater* 393:490–497
- Nowar K (2014) Peristaltic flow of a nanofluid under the effect of Hall current and porous medium. *Math Probl Eng* 389581. doi:10.1155/2014/389581
- Reddy MG, Makinde OD (2016) Magnetohydrodynamic peristaltic transport of Jeffrey nanofluid in an asymmetric channel. *J Mol Liq* 223:1242–1248
- Sarkar BC, Das S, Jana RN, Makinde OD (2015) Magnetohydrodynamic peristaltic flow of nanofluids in a convectively heated vertical asymmetric channel in presence of thermal radiation. *J Nanofluids* 4:461–473
- Shapiro AH, Jaffrin MY, Weinberg SL (1969) Peristaltic pumping with long wavelengths at low Reynolds number. *J Fluid Mech* 37:799–825
- Sheikholeslami M, Nimafar M, Ganji DD, Pouyandehmehr M (2016) $CuO - H_2O$ nanofluid hydrothermal analysis in a complex shaped cavity. *Int J Hydrog Energy* 41:17837–17845
- Sheikholeslami M, Rashidi M (2015) Effect of space dependent magnetic field on free convection of Fe_3O_4 -water nanofluid. *J Taiwan Inst Chem Eng* 56:6–15
- Srinivas S, Kothandapani M (2008) Peristaltic transport in an asymmetric channel with heat transfer. *Int Commun Heat Mass Transf* 35:514–522